Hindawi Publishing Corporation
International Journal of Photoenergy
Volume 2014, Article ID 759819, 9 pages
http://dx.doi.org/10.1155/2014/759819

Research Article

Chaos Synchronization Based Novel Real-Time Intelligent Fault Diagnosis for Photovoltaic Systems

Chin-Tsung Hsieh, Her-Terng Yau, and Jen Shiu

Department of Electrical Engineering, National Chin-Yi University of Technology, Taichung 41170, Taiwan

Correspondence should be addressed to Her-Terng Yau; pan1012@ms52.hinet.net

Received 7 December 2013; Accepted 3 January 2014; Published 18 February 2014

Academic Editor: Hongxing Yang

The traditional solar photovoltaic fault diagnosis system needs two to three sets of sensing elements to capture fault signals as fault features and many fault diagnosis methods cannot be applied with real time. The fault diagnosis method proposed in this study needs only one set of sensing elements to intercept the fault features of the system, which can be real-time-diagnosed by creating the fault data of only one set of sensors. The aforesaid two points reduce the cost and fault diagnosis time. It can improve the construction of the huge database. This study used Matlab to simulate the faults in the solar photovoltaic system. The maximum power point tracker (MPPT) is used to keep a stable power supply to the system when the system has faults. The characteristic signal of system fault voltage is captured and recorded, and the dynamic error of the fault voltage signal is extracted by chaos synchronization. Then, the extension engineering is used to implement the fault diagnosis. Finally, the overall fault diagnosis system only needs to capture the voltage signal of the solar photovoltaic system, and the fault type can be diagnosed instantly.

1. Introduction

In 2013, Hsieh and Shiu proposed a new method of the photovoltaic system fault diagnosis based on chaotic signal synchronization [1]. That method had many advantages. However, it is an offline fault diagnostic scheme. In order to improve the defect, this paper proposes the intelligent solar photovoltaic system real-time fault diagnostic device. Manual detection is replaced by the intelligent solar photovoltaic system real time fault diagnostic device. Its advantage is that, in the spacious solar photovoltaic array, as long as the output end of the array is measured and compared with previously created diagnostic data, the type of fault can be real time quickly diagnosed without manual inspection. Thus, the manual diagnosis time is shortened, while the manpower and cost losses are reduced. Therefore, this paper aims to research and develop an intelligent solar photovoltaic system real-time fault diagnostic device.

The traditional fault diagnostic device uses a neural network [1–4], Fourier analysis [5–7], or wavelet analysis [8–13] for fault diagnosis. The solar photovoltaic system fault diagnoses of different diagnostic methods are introduced below. In 2011, Shimakage et al. proposed the artificial neural network control for solar photovoltaic array fault diagnosis [14]. The diagnostic effect of the artificial neural diagnostic method proposed in that study was better than the effect of the traditional neural network. Because the authors increased the number of training layers in the neural network to three, the diagnostic effect was very good. However, an additional sensor must be mounted on each series branch solar cell to measure the voltage signal, so the cost increases with the number of solar photovoltaic arrays. In 2011, Syafaruddin et al. discussed solar photovoltaic system fault diagnosis [15]. The assumed state of the solar fault in that study is similar to that in the present study, and the diagnostic methods used in that study were measurement and observation. That study recorded the power generated by the faulted solar photovoltaic system and then compared it with the presently measured power. Although the fault diagnosis based on measurement and observation is simple, there are merely four fault types proposed by the authors. If the number of faults increases, there may be different types of faults. However, the fault category cannot be recognized in the case of identical power. In 2011, Zhao et al. proposed the fault

analysis of inverse connection of the solar photovoltaic array at low light level [16]. That study proposed the I-V curve analysis for fault diagnosis, where the condition configuration is a serial array inverse connection in the array. This condition is equivalent to a major hardware configuration error in a solar photovoltaic array that burns the line. Although the I-V curve analysis is simple and easy to implement, the observation of variance in the current costs both manpower and time. In 2012, Gokmen et al. proposed decision tree-based diagnosis of solar photovoltaic array fault types [17]. That study divided the I-V characteristic curve into four regions, whereby the regions represented four fault categories. The measured voltage and current and the voltage and current of the maximum power point were recorded, and the decision tree method was used to compare the values of the four regions. Finally, the fault category was diagnosed. The experimental results showed that, although the diagnostic rate was as high as 99.8%, the decision-making condition needed 1,637 comparisons, and the best decision-making condition was found by multiple simulations and experiments; thus, the process was very complex. In 2012, Zhao et al. proposed a simple method to diagnose solar photovoltaic systems [18]. That study used three parameter values, including the temperature coefficient of the solar cell, the illumination, and the temperature when there was a fault, to work out the variance in power, so as to diagnose the fault condition. The method only needs two simple equations to diagnose the fault condition, but the data volume of the parameters is huge, and the establishment of parameter data of various temperature and illumination changes takes considerable time. In 2013, Zhao et al. [19] proposed a new image recognition method (ICA) to identify defects in the solar cell surface. In 2013, Zhang et al. proposed the fault analysis and overcurrent protection of the solar photovoltaic array line [20].

This study used a 10-series 2-parallel solar photovoltaic array as the model of fault diagnosis. The fault condition is the short circuit set in the solar cell, and then it is diagnosed by using the chaotic synchronization signal-based fault diagnosis method, proposed in this study, and the intelligent classification of the extension theory. The chaotic system is very sensitive to change in the system, and the system parameters must change if the solar photovoltaic system has a fault. Therefore, this method only needs to import the initial value signal of the photovoltaic system with faults into the chaotic synchronization system according to the variance in initial value, to capture the variance in dynamic error, and then it is imported into the extension theory to effectively distinguish the fault state. Moreover, the extension theory does not need learning time, so the diagnosis is very rapid.

2. Solar Photovoltaic System MPPT Control

The major function of a solar photovoltaic system is to convert solar irradiation into electrical energy using a solar photovoltaic cell and an electric power converter. The equipped electric power converter can stabilize, increase, and reduce the output voltage or convert the frequency according to the requirements of the output load, and the output power depends on the area of solar photovoltaic cell, conversion efficiency, solar illumination, ambient temperature, and effect of the load. The solar photovoltaic array used in this study is a 10-series 2-parallel array, equipped with a boost converter and MPPT algorithm. This algorithm guarantees the maximum power output when the solar photovoltaic array has faults. The voltage variation is measured in the system operation to distinguish the fault.

The power characteristic generated by the solar photovoltaic cell is not linear, as the power varies with the current sunshine intensity and ambient temperature. In order to keep the output power at the maximum value of the characteristic curve, the solar photovoltaic system must be equipped with MPPT control to guarantee the maximum output power, so as to maximize the system output efficiency. At present, the common MPPT control methods are [21–25] (1) the voltage feedback method, (2) the power feedback method, (3) the straight-line approximation method, (4) the perturbation and observation method, and (5) the incremental conductance method. This paper further discusses the incremental conductance method. The extension theory is combined with this method to control the step output, which is compared with the general fixed step and the variable step.

3. Chaos Synchronization Theory and Extension Theory

3.1. Chaos Synchronization Theory. The behavior of the slave chaotic system tracking master chaotic system is chaos synchronization [26–29]. The master-slave chaotic system is described below:

$$\begin{aligned} \text{master system: } & \dot{x}(t) = f(t, x), \\ \text{slave system: } & \dot{y}(t) = f(t, y) + u(t). \end{aligned} \tag{1}$$

Among which, $x(t) = [x_1, x_2, \ldots, x_n] \in R^n$ and $y(t) = [y_1, y_2, \ldots, y_n] \in R^n$ are the status values of master system and slave system, $f : R \times R^n \rightarrow R^n$ is the nonlinear function, $B \in R^{n\times 1}$ and $C \in R^{1\times n}$, u is the controller in the slave system, and the control objective is

$$\lim_{t\to\infty} \|x(t) - y(t)\| \longrightarrow 0. \tag{2}$$

The primary fault characteristic signal in the research on solar power system fault diagnosis may be transient and fast, but the analysis of long-term signal characteristics takes much time, and too many data diagnoses are likely to cause misrecognition. Therefore, this study proposes the chaos synchronization whereby the instantaneous fault signal of the voltage is captured as the diagnostic basis of the chaotic system. Moreover, it defines the master chaotic system as the reference system and the slave chaotic system as the tracking reference system. The slave system is designed to track the reference system in a cycle length. Its tracking dynamic error convergence characteristic is used to extract dynamic error signals, and the fault feature is recorded.

3.1.1. Lorenz Chaos Synchronization System. Since the chaotic system is very sensitive to the change in system parameters, this paper specifically uses this characteristic of chaos. The solar photovoltaic system fault voltage signal is captured for chaos synchronization transformation, the trajectories of dynamic errors are extracted, and these dynamic trajectories are the fault features, so the extension theory is used to recognize fault conditions. From [1], the Lorenz chaos synchronization system is expressed as (3)

$$\begin{aligned} \text{master}: &\begin{cases} \dot{x}_1 = \alpha\left(x_2 - x_1\right), \\ \dot{x}_2 = \beta x_1 - x_1 x_3 - x_2, \\ \dot{x}_3 = x_1 x_2 - \gamma x_3, \end{cases} \\ \text{slave}: &\begin{cases} \dot{y}_1 = \alpha\left(y_2 - y_1\right) + u_1, \\ \dot{y}_2 = \beta y_1 - y_1 y_3 - y_2 + u_2, \\ \dot{y}_3 = y_1 y_2 - \gamma y_3 + u_3. \end{cases} \end{aligned} \tag{3}$$

The master-slave system error state can be expressed as $e_1 = x_1 - y_1$, $e_2 = x_2 - y_2$, and $e_3 = x_3 - y_3$; the dynamic error system is (4). The slave system tracking master system is observed, so that the control signal is chosen as $u_1 = u_2 = u_3 = 0$.

$$\begin{bmatrix} \dot{e}_1 \\ \dot{e}_2 \\ \dot{e}_3 \end{bmatrix} = \begin{bmatrix} -\alpha & \alpha & 0 \\ \beta & -1 & 0 \\ 0 & 0 & -\gamma \end{bmatrix} \begin{bmatrix} e_1 \\ e_2 \\ e_3 \end{bmatrix} + \begin{bmatrix} 0 \\ y_1 y_3 - x_1 x_3 \\ -y_1 y_2 + x_1 x_2 \end{bmatrix}. \tag{4}$$

According to [1], if the eigenvalue of the system is negative, the error system state is steady, so the chaotic attractor can be generated, and the dynamic trajectory of the chaotic attractor is used for various studies. This paper observes the dynamic trajectory of the chaotic attractor to distinguish the fault types of the solar photovoltaic system.

3.2. Extension Theory. The extension theory can solve the compatibility and contradictory problems, it describes the quality of things quantitatively without learning, and it has high accuracy. Based on the aforesaid characteristics, it is very suitable for classification recognition. This paper therefore uses extension theory as the solar photovoltaic system fault diagnosis method.

3.2.1. Definition of Extension Matter Element. In order to distinguish the differences among things, names are assigned. The extension can use the matter-element concept to present the differences among things in the matter-element model, expressed as [30]

$$R = (N, C, V) = \begin{bmatrix} N & c_1 & v_1 \\ & c_2 & v_2 \\ & \vdots & \vdots \\ & c_n & v_n \end{bmatrix}, \tag{5}$$

where N is the matter, c_j is the characteristic of the matter, and v_j is the value of the characteristic c_j.

3.2.2. Definition of the Extension Set. In classical mathematics, the classical set uses 0 and 1 to describe the characteristics of things, whereas, in fuzzy mathematics, the fuzzy set uses 0 to 1 to describe the fuzzy degree of characteristics of things. The extension set extends the range of the set to $-\infty$ to ∞ to represent the extension degree of the characteristics of things. The extension correlation function is of two intervals in the real number field $\langle -\infty, \infty \rangle$, which are the classical domain $S_o = \langle a, b \rangle$ and the joint domain $S_p = \langle c, d \rangle$, and interval $S_o \in S_p$. If there is a random point s in the real number field, the correlation function can be described as (6), and the overall extension set correlation grade can be expressed as in Figure 1:

$$\begin{aligned} D = \left(s, S_o, S_p\right) &= \begin{cases} \rho\left(s, S_p\right) - \rho\left(s, S_o\right), & s \notin S_o, \\ -1, & s \in S_o, \end{cases} \\ K(s) &= \frac{\rho\left(s, S_o\right)}{D\left(s, S_o, S_p\right)}, \end{aligned} \tag{6}$$

where

$$\begin{aligned} \rho\left(s, S_o\right) &= \left| s - \frac{a+b}{2} \right| - \frac{b-a}{2} \\ \rho\left(s, S_p\right) &= \left| s - \frac{c+d}{2} \right| - \frac{d-c}{2}, \end{aligned} \tag{7}$$

where $K(s)$ is the grade of correlation between s and S_o. When $K(s) \geqq 0$, it is the degree of s belonging to S_o; when $K(s) < 0$, it is the degree of s not belonging to S_o.

3.3. Diagnostic Process Architecture of the Chaos Synchronization System and Extension Diagnosis. Figure 2 is the chaotic signal synchronization and extension diagnostic system flow chart. First, the measured voltage of the solar photovoltaic system is recorded, and then the recorded voltage signal to be measured is imported into the slave system of the chaotic signal synchronization system. The chaotic synchronization system then generates the chaotic dynamic error signal after subtraction between the master and slave systems, and the dynamic trajectory formed of the chaotic dynamic error signal is the main basis of extension diagnosis, that is, the fault feature of the solar photovoltaic system. Finally, as long as the chaotic dynamic error signal is imported into the finished extension matter-element model, the fault category can be identified rapidly and accurately by extension diagnosis of the fault conditions.

4. Experimental Results

4.1. Extension Incremental Conductance Method. In terms of the solar photovoltaic system MPPT, this paper proposes the extension incremental conductance method (EICM) and compares it with the general fixed step incremental conductance method (FICM) and the variable step incremental conductance method (VICM). As the fixed step incremental conductance method has only one set of steps (step = 0.001), the tracking speed is always the same whatever the dP/dV is.

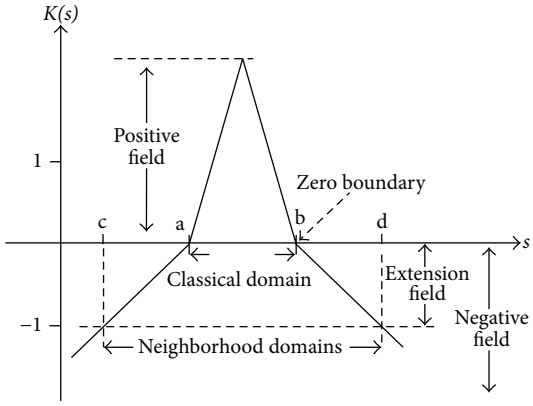

Figure 1: Schematic diagram of the correlation function.

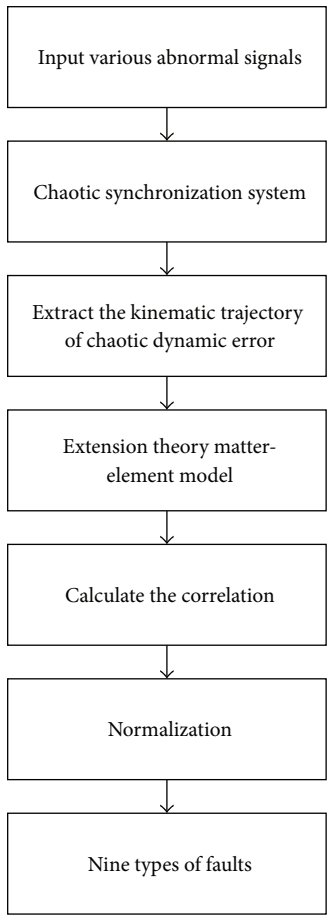

Figure 2: Chaotic signal synchronization and extension diagnostic system flow chart.

Neither the speed nor the step can be adjusted, which becomes the main defect in the most fundamental incremental conductance method. The variable step incremental conductance method has large steps (step = 0.005) and small steps (step = 0.001), and its tracking speed is much higher than that of the general fixed step incremental conductance method, but the dP/dV identification mode is not intelligent enough. The extension incremental conductance method proposed in this paper can extend the matter-element model according to the dP/dV value and reach intelligent identification and rapid tracking under the same condition (step = 0.005 and 0.001). The result is shown in Figure 3. The classical domain and joint domain of the extension incremental conductance method are shown in Table 1.

Table 1: Matter-element model of the extension incremental conductance method for dP/dV.

[Joint domain, c_1, $\langle 0, 10000\rangle$]
[Large step, c_1, $\langle 5.0001, 10000\rangle$]
[Small step, c_1, $\langle 0, 5\rangle$]

Table 2: Solar panel model and specifications.

Solar panel model	SM 1611
Open circuit voltage	3.0 V
Short circuit current	0.8 A
Maximum power point voltage	2.36 V
Maximum power point current	0.7 A
Maximum power	1.65 W

Table 3: Solar photovoltaic system fault category.

Fault type	Fault condition (short circuit set in faulted solar cell)
SCF_1	There is no fault in the two-series branch solar photovoltaic system.
SCF_2	One solar cell fault occurs in any series branch of the two-series branch solar photovoltaic system.
SCF_3	Two solar cell faults occur in any series branch of the two-series branch solar photovoltaic system.
SCF_4	Three solar cell faults occur in any series branch of the two-series branch solar photovoltaic system.
SCF_5	One solar cell fault occurs in each series branch of the two-series branch solar photovoltaic system.
SCF_6	Two solar cell faults occur in each series branch of the two-series branch solar photovoltaic system.
SCF_7	One solar cell fault occurs in one series branch and two solar cell faults occur in the other branch of the two-series branch solar photovoltaic system.
SCF_8	One solar cell fault occurs in one series branch and four solar cell faults occur in the other branch of the two-series branch solar photovoltaic system.
SCF_9	Two solar cell faults occur in one series branch and three solar cell faults occur in the other branch of the two-series branch solar photovoltaic system.

4.2. Implementation of the Solar Photovoltaic System Real-Time Fault Diagnosis. The solar cell in this paper is SM 1611; its specifications are shown in Table 2. The solar illumination is 1,000 W/m^2, and the ambient temperature is 25°C. The system architecture is shown in Figure 4. The connection mode is 10-series 2-parallel, as shown in Figure 5. The fault state should be simulated before the fault condition is diagnosed. The fault types are shown in Table 3 [31, 32]. The V-P

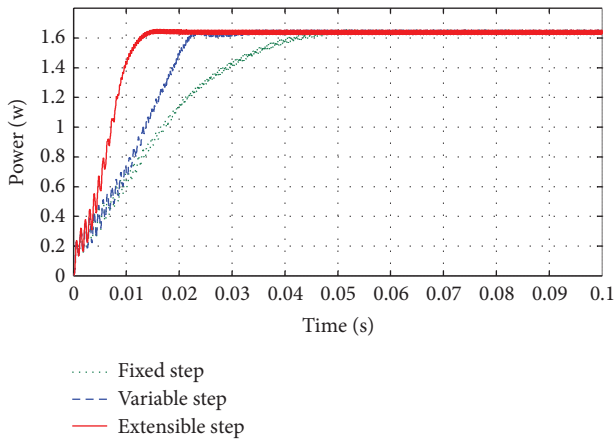

Figure 3: Comparison result of FICM, VICM, and EICM.

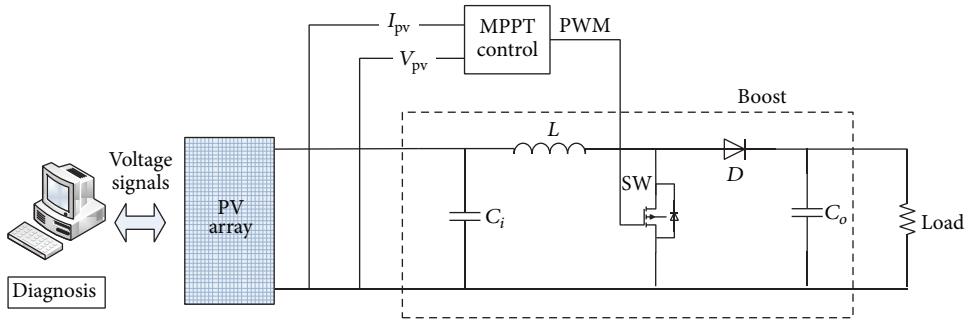

Figure 4: System architecture of the solar photovoltaic system.

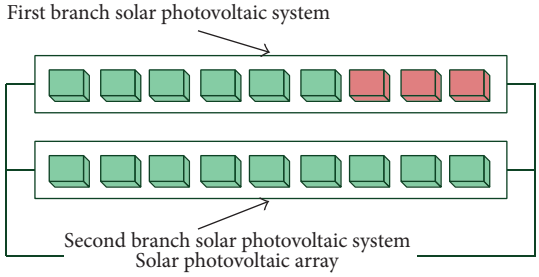

Figure 5: Schematic diagram of faults in the solar photovoltaic array (SCF_7).

and V-I characteristic curves of the solar photovoltaic array vary with the sunshine and ambient temperature. The fault condition in this paper is the short circuit set in the solar panel, and nine kinds of solar cell fault (SCF) are simulated. Therefore, there are nine kinds of V-P and V-I characteristic curves, as shown in Figures 6(a) and 6(b). The fault voltage signal is mixed with a minute quantity of Gaussian noise, as shown in Figure 7. The maximum power point voltage when a fault occurs is measured and recorded, as shown in Figure 8. The addition of Gaussian noise is helpful in enlarging the dynamic trajectory of chaotic dynamic error, so as to highlight the fault feature; meanwhile the tolerance of the system for noise can be written in the extension matter-element model, so that the system can resist noise. Finally, as long as the nine kinds of fault voltage signal are imported into the chaos synchronization system, the fault features can be extracted as the base of extension matter-element modeling. The environment noise of a physical system is usually a high frequency signal. Therefore, a low-pass filter could be used to pretreat the system signal.

The solar photovoltaic array for this experiment is the Agilent Technologies E4360A modular solar array platform. When the nine fault characteristic curves of solar energy in Figures 6(a) and 6(b) are imported into the E4360A modular solar array platform, nine fault voltages can be exported. The MPPT algorithm is implemented by dSPACE and is finally connected to the boost converter to record the voltages of various fault conditions for fault diagnosis. Figure 8 shows the measured voltage with Gaussian noise. The experimental sampling rate is 10 kHz. The master system of the chaos synchronization system bears the normal voltage signal of the solar photovoltaic system, and the slave system bears the faulted voltage signal of the solar photovoltaic system. The unmeasured voltage signal is imported into the chaos synchronization system of (1) the chaos synchronization error is converted into dynamic error to obtain the $\dot{e}_1\dot{e}_2\dot{e}_3$ three-dimensional motion trajectory, as shown in Figure 9.

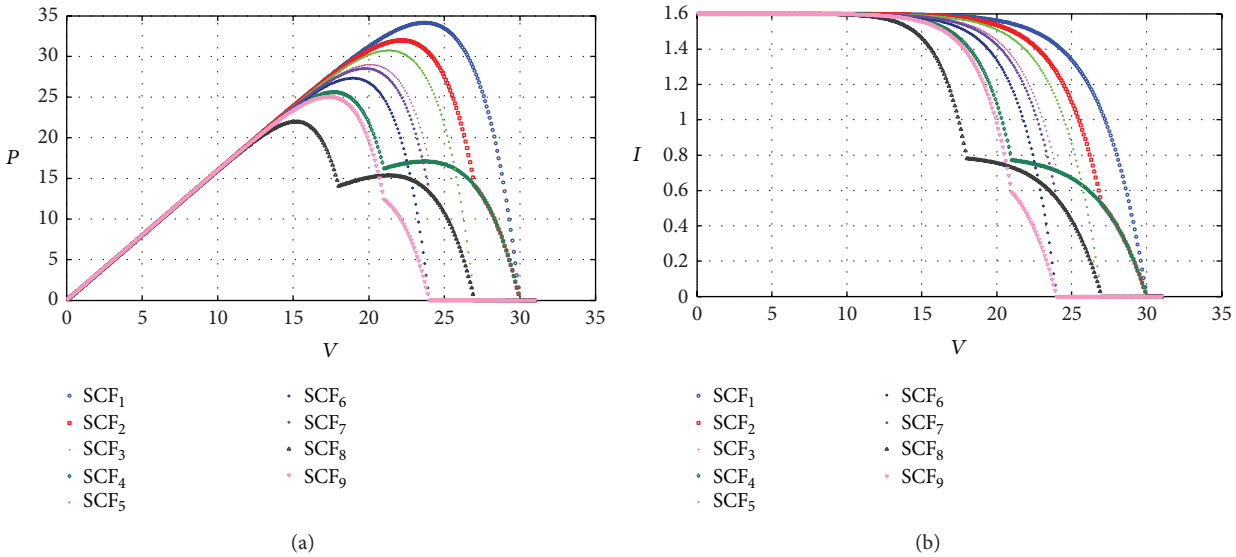

Figure 6: (a) V-P characteristic curves of nine faults. (b) V-I characteristic curves of nine faults.

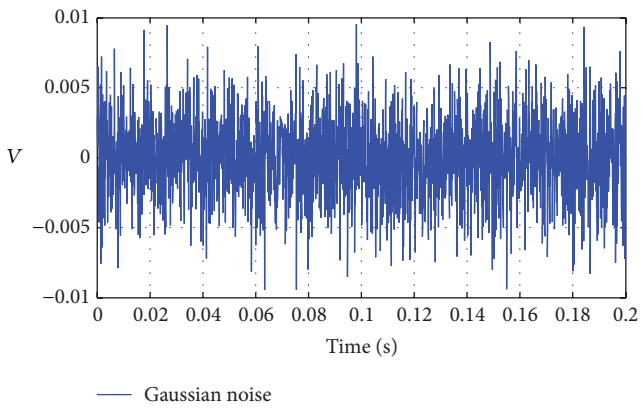

Figure 7: Gaussian noise (0.1%).

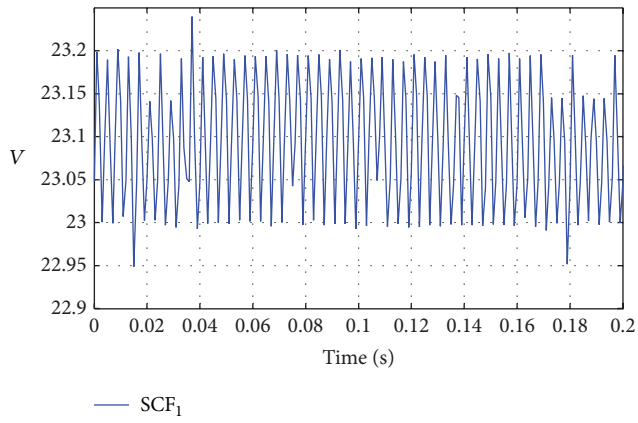

Figure 8: Voltage signal of SCF_1 with Gaussian noise.

The plan view of the dynamic error of the nine faults is shown in Figure 9.

The nine patterns are put on the same plane. The dynamic trajectory of each fault is shown in Figure 10. The chaotic dynamic trajectory is used to build the extension matter-element model. Figure 10 shows the chaotic waveform circle 0 of $\dot{e}_1$, which tends to be symmetrical. As the chaotic dynamic trajectory of $\dot{e}_1$ in $\langle -2, -0\rangle$ and $\langle 0, 2\rangle$ intervals is very apparent, $\dot{e}_1$ in $\langle -2, 0\rangle$ and $\langle 0, 2\rangle$ intervals is used as the basis of the extension matter. The $\dot{e}_3$ corresponding to $\dot{e}_1$ interval landing point is calculated, and the average of $\dot{e}_3$ landing point is extracted as the eigenvalue extracted in this paper. The matter-element model is shown in Table 4. The weight in this paper is set as 0.5. The solar photovoltaic system can be diagnosed after the extension matter-element model is built.

If the fault diagnosis cannot implement real-time measurement and diagnosis, it wastes both time and money. Therefore, this study implemented real-time fault diagnosis of the solar photovoltaic system, saving a considerable amount of time. The fault state displayed by the diagnostic system needs to be considered. The real-time fault diagnosis system is implemented using the dSPACE hardware system, the system sampling rate is 10 kHz, and the diagnosis is renewed when the number of data is 10,000; that is, the diagnostic values are updated per second. Therefore, the fault diagnosis system needs only one second to diagnose the faults in the solar photovoltaic system, so as to implement real-time diagnosis. Figure 11 shows the system hardware facilities. Figure 12 shows the real-time diagnosis interface of dSPACE. In the experiment of real-time diagnosis, this paper measured the nine faults 20 times, respectively. Meanwhile five percentages of Gaussian noise (0.1%, 0.3%, 0.5%, 1%, and 5%) were added in to test the real-time diagnosis rate of the system and to test the tolerance of the diagnostic system with the noise. Table 5 shows the real-time diagnosis rate.

In the traditional fault diagnosis system, once there is a little noise interference, the diagnosis will be inaccurate.

Table 4: Chaotic dynamic trajectory matter-element model.

Neighborhood domains $=$	$\begin{bmatrix} \text{Normal} & c_1 & \langle 200, 500\rangle \\ & c_2 & \langle 200, 500\rangle \end{bmatrix}$	$\text{SCF}_1 = \begin{bmatrix} \text{Fault} & c_1 & \langle 460, 480\rangle \\ & c_2 & \langle 460, 480\rangle \end{bmatrix}$
$\text{SCF}_2 = \begin{bmatrix} \text{Fault} & c_1 & \langle 430, 450\rangle \\ & c_2 & \langle 430, 450\rangle \end{bmatrix}$		$\text{SCF}_3 = \begin{bmatrix} \text{Fault} & c_1 & \langle 380, 390\rangle \\ & c_2 & \langle 380, 390\rangle \end{bmatrix}$
$\text{SCF}_4 = \begin{bmatrix} \text{Fault} & c_1 & \langle 310, 320\rangle \\ & c_2 & \langle 310, 320\rangle \end{bmatrix}$		$\text{SCF}_5 = \begin{bmatrix} \text{Fault} & c_1 & \langle 410, 420\rangle \\ & c_2 & \langle 410, 420\rangle \end{bmatrix}$
$\text{SCF}_6 = \begin{bmatrix} \text{Fault} & c_1 & \langle 340, 360\rangle \\ & c_2 & \langle 340, 360\rangle \end{bmatrix}$		$\text{SCF}_7 = \begin{bmatrix} \text{Fault} & c_1 & \langle 370, 375\rangle \\ & c_2 & \langle 370, 375\rangle \end{bmatrix}$
$\text{SCF}_8 = \begin{bmatrix} \text{Fault} & c_1 & \langle 230, 250\rangle \\ & c_2 & \langle 230, 250\rangle \end{bmatrix}$		$\text{SCF}_9 = \begin{bmatrix} \text{Fault} & c_1 & \langle 295, 307\rangle \\ & c_2 & \langle 295, 307\rangle \end{bmatrix}$

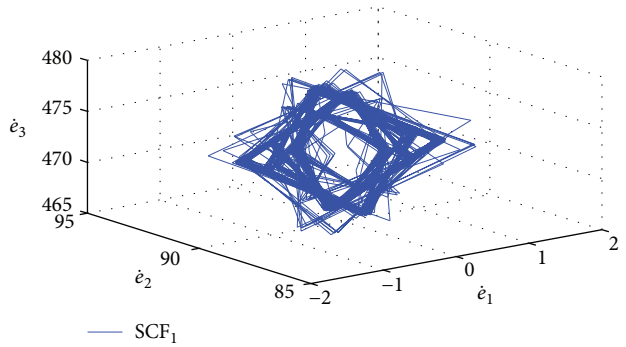

Figure 9: Three-dimensional diagram of $\dot{e}_1\dot{e}_2\dot{e}_3$ dynamic error of SCF_1.

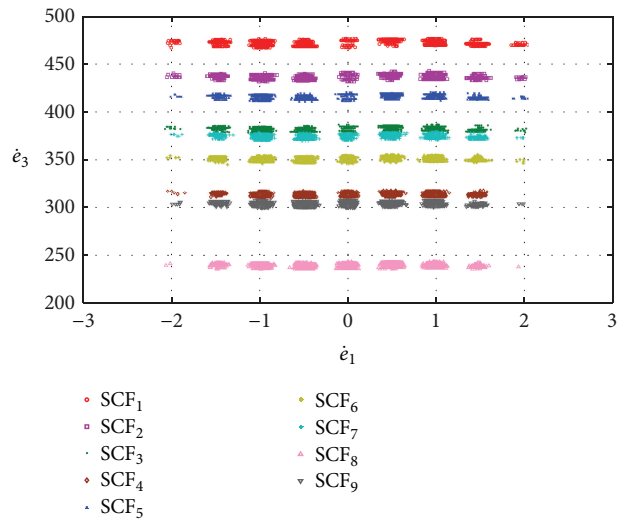

Figure 10: Plan view of $\dot{e}_1$–$\dot{e}_3$ dynamic errors of SCF_1–SCF_9.

However, in the chaotic system, not only does a little noise make the dynamic error trajectory more apparent, but also the system can tolerate the noise interference. Therefore, the diagnostic system in this paper resists noise, and its diagnostic rate is still high when the noise changes drastically.

Table 5: Real-time diagnosis rate.

Percentage of additional Gaussian noise (%)	Number of intercepted real-time diagnostic signals (signals)	Diagnostic rate (%)
0.1	180	100
0.3	180	100
0.5	180	100
1	180	100
5	180	98.89

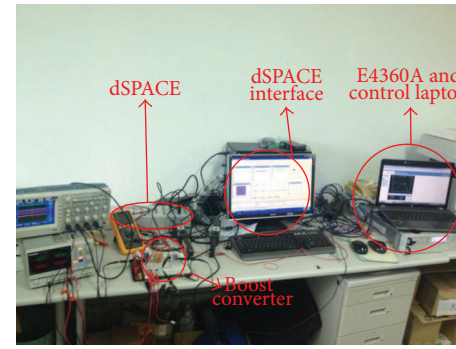

Figure 11: System hardware facilities.

5. Conclusions

The paper derived a real-time system to diagnose the faults in a solar photovoltaic system. The chaos synchronization and extension theory were used to distinguish the fault types. The extension theory does not need to create too much data, and neither does it require training or learning. Its diagnosis is very fast in comparison with general neural diagnosis. This method proposed in this paper only needs one set of sensors to capture a voltage signal, which is then imported into the chaos synchronization system. In the dynamic error graph of the chaos synchronization system converted from voltage signals, accurate, rapid, timesaving, and cost saving fault recognition can be implemented only by capturing two fault features. In comparison with other traditional fault diagnosis methods which need at least three sensor modules to capture the physical quantities before system diagnosis,

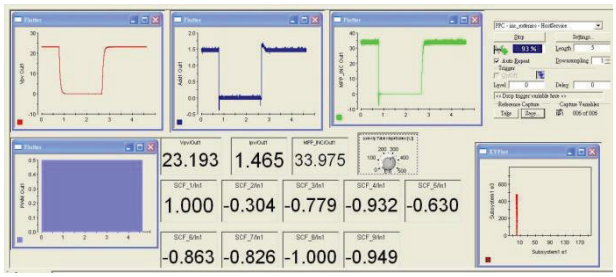

Figure 12: dSPACE real-time diagnosis interface.

the fault diagnostic device of this paper can save the cost of sensors while implementing real-time diagnosis. As an intelligent fault diagnostic device, its diagnosis is very rapid and accurate.

Conflict of Interests

The authors declare no conflict of interests regarding the publication of this paper.

References

[1] C. T. Hsieh and J. Shiu, "Study of intelligent photovoltaic system fault diagnostic scheme based on chaotic signal synchronization," *Mathematical Problems in Engineering*, vol. 2013, Article ID 816296, 6 pages, 2013.

[2] H. Guolian, J. Pan, W. Zhentao, and Z. Jianhua, "Research on fault diagnosis of wind turbine control system based on Artificial Neural Network," in *Proceedings of the 8th World Congress on Intelligent Control and Automation (WCICA '10)*, pp. 4875–4879, Jinan, China, July 2010.

[3] H. Fang and C. Xia, "A fuzzy neural network based fault detection scheme for synchronous generator with internal fault," in *Proceedings of the 6th International Conference on Fuzzy Systems and Knowledge Discovery (FSKD '09)*, pp. 433–437, Tianjin, China, August 2009.

[4] G. Xiong, D. Shi, L. Zhu, and X. Duan, "A new approach to fault diagnosis of power systems using fuzzy reasoning spiking neural p systems," *Mathematical Problems in Engineering*, vol. 2013, Article ID 815352, 13 pages, 2013.

[5] M. Pineda-Sanchez, M. Riera-Guasp, J. A. Antonino-Daviu, J. Roger-Folch, J. Perez-Cruz, and R. Puche-Panadero, "Diagnosis of induction motor faults in the fractional fourier domain," *IEEE Transactions on Instrumentation and Measurement*, vol. 59, no. 8, pp. 2065–2075, 2010.

[6] J. H. Lee, Y. K. Seong, C. H. Chang et al., "Fourier-based shape feature extraction technique for computer-aided b-mode ultrasound diagnosis of breast tumor," in *Proceedings of the Annual International Conference of the IEEE Engineering in Medicine and Biology Society (EMBC'12)*, pp. 6551–6554, San Diego, Calif, USA, August 2012.

[7] E. Uslu and G. Bilgin, "Exploiting locality based Fourier transform for ECG signal diagnosis," in *Proceedings of the International Conference on Applied Electronics (AE'12)*, pp. 323–326, Pilsen, Czech Republic, September 2012.

[8] K. Li, P. Chen, and H. Wang, "Intelligent diagnosis method for rotating machinery using wavelet transform and ant colony optimization," *IEEE Sensors Journal*, vol. 12, no. 7, pp. 2474–2484, 2012.

[9] A. Bouzida, O. Touhami, R. Ibtiouen, A. Belouchrani, M. Fadel, and A. Rezzoug, "Fault diagnosis in industrial induction machines through discrete wavelet transform," *IEEE Transactions on Industrial Electronics*, vol. 58, no. 9, pp. 4385–4395, 2011.

[10] J. Pons-Llinares, J. A. Antonino-Daviu, M. Riera-Guasp, M. Pineda-Sanchez, and V. Climente-Alarcon, "Induction motor diagnosis based on a transient current analytic wavelet transform via frequency B-Splines," *IEEE Transactions on Industrial Electronics*, vol. 58, no. 5, pp. 1530–1544, 2011.

[11] Q. Liu, F. Chen, Z. Zhou, and Q. Wei, "Fault diagnosis of rolling bearing based on wavelet package transform and ensemble empirical mode decomposition," *Advances in Mechanical Engineering*, vol. 2013, Article ID 792584, 6 pages, 2013.

[12] G. Campetelli, D. Zumoffen, and M. Basualdo, "Improvements on noninvasive blood glucose biosensors using wavelets for quick fault detection," *Journal of Sensors*, vol. 2011, Article ID 368015, 11 pages, 2011.

[13] W. Li, Z. Wang, Z. Zhu, G. Zhou, and G. Chen, "Design of online monitoring and fault diagnosis system for belt conveyors based on wavelet packet decomposition and support vector machine," *Advances in Mechanical Engineering*, vol. 2013, Article ID 797183, 10 pages, 2013.

[14] T. Shimakage, K. Nishioka, H. Yamane, M. Nagura, and M. Kudo, "Development of fault detection system in PV system," in *Proceedings of the 33rd International Telecommunications Energy Conference (INTELEC'11)*, Amsterdam, The Netherlands, October 2011.

[15] S. Syafaruddin, E. Karatepe, and T. Hiyama, "Controlling of artificial neural network for fault diagnosis of photovoltaic array," in *Proceedings of the IEEE 33rd International Telecommunications Energy Conference (INTELEC'11)*, pp. 1–5, Amsterdam, The Netherlands, September 2011.

[16] Y. Zhao, B. Lehman, J. F. De Palma, J. Mosesian, and R. Lyons, "Fault analysis in solar PV arrays under: low irradiance conditions and reverse connections," in *Proceedings of the 37th IEEE Photovoltaic Specialists Conference (PVSC'11)*, pp. 2000–2005, Seattle, Wash, USA, June 2011.

[17] N. Gokmen, E. Karatepe, B. Celik, and S. Silvestre, "Simple diagnostic approach for determining of faulted PV modules in string based PV arrays," *Solar Energy*, vol. 86, no. 11, pp. 3364–3377.

[18] Y. Zhao, L. Yang, B. Lehman, J.-F. De Palma, J. Mosesian, and R. Lyons, "Decision tree-based fault detection and classification in solar photovoltaic arrays," in *Proceedings of the 27th Annual IEEE Applied Power Electronics Conference and Exposition (APEC'12)*, pp. 93–99, Orlando, Fla, USA, February 2012.

[19] Y. Zhao, J. F. De Palma, J. Mosesian, R. Lyons, and B. Lehman, "Line-line fault analysis and protection challenges in solar photovoltaic arrays," *IEEE Transactions on Industrial Electronics*, vol. 60, no. 9, pp. 3784–3795, 2013.

[20] X. Zhang, H. Sun, Y. Zhou, J. xi, and M. Li, "A novel method for surface defect detection of photovoltaic module based on independent component analysis," *Mathematical Problems in Engineering*, vol. 2013, Article ID 520568, 8 pages, 2013.

[21] H. Wu and X. Tao, "Three phase photovoltaic grid-connected generation technology with MPPT function and voltage control," in *Proceedings of the International Conference on Power Electronics and Drive Systems (PEDS'09)*, pp. 1295–1300, Taipei, Taiwan, January 2009.

[22] M. A. Elgendy, B. Zahawi, and D. J. Atkinson, "Assessment of perturb and observe MPPT algorithm implementation techniques for PV pumping applications," *IEEE Transactions on Sustainable Energy*, vol. 3, no. 1, pp. 21–33, 2012.

[23] F. Liu, S. Duan, F. Liu, B. Liu, and Y. Kang, "A variable step size INC MPPT method for PV systems," *IEEE Transactions on Industrial Electronics*, vol. 55, no. 7, pp. 2622–2628, 2008.

[24] Q. Mei, M. Shan, L. Liu, and J. M. Guerrero, "A novel improved variable step-size incremental-resistance MPPT method for PV systems," *IEEE Transactions on Industrial Electronics*, vol. 58, no. 6, pp. 2427–2434, 2011.

[25] H. T. Yau, C. J. Lin, and C. H. Wu, "Sliding mode extremum seeking control scheme based on PSO for maximum power point tracking in photovoltaic systems," *International Journal of Photoenergy*, vol. 2013, Article ID 527948, 10 pages, 2013.

[26] C. Bianca and L. Rondoni, "The nonequilibrium ehrenfest gas: a chaotic model with flat obstacles?" *Chaos*, vol. 19, no. 1, Article ID 013121, 2009.

[27] C. Bianca, "Weyl-flow and the conformally symplectic structure of thermostatted billiards: the problem of the hyperbolicity," *Nonlinear Analysis: Hybrid Systems*, vol. 5, no. 1, pp. 32–51, 2011.

[28] H.-T. Yau, "Generalized projective chaos synchronization of gyroscope systems subjected to dead-zone nonlinear inputs," *Physics Letters A*, vol. 372, no. 14, pp. 2380–2385, 2008.

[29] H.-T. Yau, C.-C. Wang, C.-T. Hsieh, and C.-C. Cho, "Nonlinear analysis and control of the uncertain micro-electro-mechanical system by using a fuzzy sliding mode control design," *Computers and Mathematics with Applications*, vol. 61, no. 8, pp. 1912–1916, 2011.

[30] M. H. Wang, "Application of extension theory to vibration fault diagnosis of generator sets," *IEE Proceedings Generation Transmission and Distribution*, vol. 151, no. 4, pp. 503–508, 2004.

[31] K.-H. Chao, S.-H. Ho, and M.-H. Wang, "Modeling and fault diagnosis of a photovoltaic system," *Electric Power Systems Research*, vol. 78, no. 1, pp. 97–105, 2008.

[32] K.-H. Chao, C.-T. Chen, M.-H. Wang, and C.-F. Wu, "A novel fault diagnosis method based-on modified neural networks for photovoltaic systems," in *Advances in Swarm Intelligence*, vol. 6146 of *Lecture Notes in Computer Science*, pp. 531–539, Springer, Berlin, Germany, 2010.